DOI: 10.1021/cg901593x

CRYSTAL GROWTH & DESIGN Article

2010, Vol. 10
3391–3396

Toward the Crystallization of Photosystem II Core Complex from *Pisum sativum* L.

T. Prudnikova,[†] J. A. Gavira,[‡] P. Řezáčová,[§] E. Pineda Molina,[‡] I. Hunalová,[#] E. Sviridova,[†] V. Shmidt,[†] J. Kohoutová,[†] M. Kutý,[†,∥] D. Kaftan,[†] F. Vácha,[†,#] J. M. García-Ruiz,[‡] and I. Kutá Smatanová*[,†,∥]

[†]*Institute of Physical Biology, University of South Bohemia in České Budějovice, Zámek 136, 373 33 Nové Hrady, Czech Republic,* [‡]*Laboratorio de Estudios Cristalográficos, Edf. López Neyra, P.T. Ciencias de la Salud, Avenida del Conocimiento s/n, 18100 Armilla (Granada) Spain,* [§]*Institute of Molecular Genetics of the Academy of Science of the Czech Republic, v.v.i., Flemingovo no. 2, 16637 Prague, Czech Republic,* [#]*Biology Centre of the Academy of Science of the Czech Republic, v.v.i., Institute of Plant Molecular Biology, Branišovská 31, 370 05 České Budějovice, Czech Republic, and* [∥]*Institute of Systems Biology and Ecology of the Academy of Science of the Czech Republic, v.v.i., Zámek 136, 373 33 Nové Hrady, Czech Republic*

Received December 18, 2009; Revised Manuscript Received May 20, 2010

ABSTRACT: The crystallization of the higher plant ~1 gigadalton homodimeric lipid-pigment−protein complex of photosystem II constitutes a challenging undertaking that has not been crowned with success to date. In the continuation of our previous efforts (Kuta-Smatanova et al. *Photosyn. Res.* **2006**, *90*, 255−259) that had provided needle and plate crystals of plant photosystem II for the first time, we report on a study to crystallize three-dimensional crystals of the photosystem II from *Pisum sativum* L. suitable for X-ray analysis. In our screening, we optimized temperature, supersaturation rate, and concentrations of detergents, buffers, salts, and organic additives. We used a sitting and hanging drop vapor-diffusion method, microbatch under oil and counter-diffusion techniques, and direct and cross-influenced procedures. We have identified that the major limiting factors for the growth of crystals are the photosystem II stability and requirement of indispensable divalent cations. The newly proposed physicochemical conditions also take into account its liability toward the oxidative stress, temperature, and light sensitivity.

Introduction

The photosystem II (PSII) complex is located in the thylakoid membranes of prokaryotic cyanobacteria and chloroplasts of higher plants and algae.[1,2] In the process of photosynthesis, the PSII uses light energy to couple the oxidation of water and hence the production of molecular oxygen to the generation of the reduction potential for the fixation of atmospheric carbon dioxide and the resulting biomass production.[3,4] Both the aerobic atmosphere and the readily usable carbon source are the essential elements that sustain almost all life forms on Earth. The exploitation of nature's inventions for our future biotechnological applications that may provide sustained energy and food resources requires our understanding of the photosynthetic process in great detail and the knowledge of the PSII function and its structure on an atomic level in particular. Perhaps the most enigmatic biochemical process known to date is catalyzed by the oxygen evolving complex (OEC) at the donor side of the PSII. Elucidation of the structure of the OEC will have far reaching consequences beyond our mere understanding of the mechanism of water splitting. To yield a high resolution structure of PSII, X-ray crystallography has been applied with a partial success for determination of several structures of thermophilic cyanobacterial PSII[5−12] to the maximum resolution attained at 2.9 Å.[13] Still, the fine structure of the OEC has not been resolved even in the thermophilic systems, and no crystal structure of PSII from higher plants is available whatsoever. The medium resolution models of plant PSII based on the data from single particle electron microscopy have been however available for two decades.[14−16] A close picture of the PSII−LHCII supercomplexes with variable antenna sizes, ranging from the sole PSII core to the large $C_2S_2M_2$ supercomplex, has been presented recently by Caffarri and co-workers[17] with a stunning resolution of 12.0 Å.

The reasons behind the poor success with obtaining a high resolution structure of plant PSII either through electron microscopy or even more the X-ray crystallography are the PSII massive size, its structure complexity, the complexes' heterogeneity, and their impermanence. Each of the two monomers of the PSII core complex ($PSII_{CC}$) consists of the integral membrane subunits D1, D2 and cytochrome *b* 559 creating the photochemical reaction center (RC), the membrane bound inner antenna pigment−protein complexes CP43 and CP47, and at least 17 additional low molecular mass membrane subunits (< 10 kDa) of mostly unknown functions. In higher plants, the four extrinsic proteins (PsbO, PsbP, PsbQ, PsbR) of the OEC[18] are essential to keep the manganese complex integrity through its binding to PsbO as well as to drive oxygen production.[11] The ~35 chlorophyll *a* molecules, over 10 carotenoids, quinone molecules (Q_A and Q_B) and a host of inorganic ions (Ca^{2+}, Cl^-, Mn^{3+}, Mg^{2+}, Fe^{2+}, HCO^{3-}) coordinated by specific residues of the PSII proteins along with redox-active groups (e.g., D1-Tyr161), serve for light harvesting, light transformation, electron transport, and water splitting. It is expected that the $PSII_{CC}$ is also associated with numerous lipid molecules originating from thylakoid membrane that will play various structural and functional roles akin to those proposed for the PSII of cyanobacteria.[12,13,19]

*Corresponding author; tel: +420608106109, fax: +420386361219, e-mail: ivas@ufb.jcu.cz (ivanaks@seznam.cz).

Published on Web 06/22/2010

To resolve this complicated structure at high resolution, we set our hopes on the X-ray crystallography as the only candidate technique that may deliver it. The conditions for a successful crystallization of macromolecules are in general devised by tedious screening of vast counts of chemical (precipitants, additives, pH, etc.) and physical (temperature, vapor diffusion rate, etc.) parameters as well as standard and advanced crystallization methods. However, most combinations of the physicochemical conditions may prevent the crystallization by promoting heterogeneity of the conformational, oligomeric, etc. states of the macromolecular complexes.[9,20,21] In membrane protein complexes, such as the $PSII_{CC}$, the presence of specific detergents will also affect the protein complexes' homogeneity since the complexes have to be solubilized prior to the setup of the crystallization trials. Conceivably, the most prominent setbacks are the temperature and light sensitivity of the $PSII_{CC}$ and its susceptibility to oxidation, which are the source of the breakdown of the complexes, induce their heterogeneity, and prevent formation of well-ordered crystals. To minimize the complexes' light induced oxidation, blue and red light have to be avoided during the whole process from purification to crystallization. Instead, a dim green ambient light and a microscope equipped with green light filters have to be used.

Here we review the efforts to crystallize plant PSII in the past decades and give an account of our own progress toward the highly diffracting crystals of $PSII_{CC}$. We have applied the previously reported crystallization conditions to crystallize $PSII_{CC}$ from green pea *Pisum sativum* L. employing traditional and modern crystallization techniques to a limited success. We have identified the chemical and physical factors that promote the crystal growth in 3D as well as those that preclude the successful crystallization. Our knowledge based design of screening for the effect of different additives on the crystallization yielded considerable advancement in crystal quality although currently standing at 10.0 Å resolution.

Experimental Section

Isolation of PSII Enriched Thylakoid Membranes. PSII was isolated according to Ghanotakis[22] under green light at 4 °C using an improved procedure described by Kern and co-worker[7] with our modifications. Whole shoots of *Pisum sativum* L. var. 'Radovan' plants grown under ambient light on vermiculite were cut and homogenized in a blender with 0.5 L of the Grind medium (50 mM of KH_2PO_4, 0.35 M of KCl, 0.5 mM Na-EDTA, pH 7.5), the filtrated slurry was centrifuged for 15 min at 7000 g, the pellet was resuspended in the SNT buffer (0.2 M of sacharose, 0.1 mol of NaCl, 50 mM tricine, 50 mM $MgCl_2$, pH 8.0) and centrifuged for 15 min at 7000*g*, and the pellet was resuspended in the HSB buffer (5 mM $MgCl_2$, 15 mM NaCl, 2 mM 2-(*N*-morpholino)ethanesulfonic acid (MES) NaOH, pH 6.3) five times homogenized in a glass homogenizer, diluted to final concentration of 3 mg of chlorophyll *a* (Chl *a*) mL^{-1}, and stirred on ice for 30 min. Then, 10% Triton in the HSB buffer was added to yield a final concentration of 2 mg (Chl *a*) mL^{-1} while the solution was stirred for another 30 min on ice. The suspension was then centrifuged for 35 min at 40000*g*. The pellet was resuspended in the Magic buffer (5 mM $MgCl_2$, 15 mM NaCl, 10% glycerol (w:v), 20 mM MES NaOH, pH 6.3) and centrifuged for 20 min at 40000*g*. The pellet was resuspended in a small volume of the Magic buffer and homogenized five times in a glass homogenizer. This BBY sample of a final concentration of 3 mg (Chl *a*) mL^{-1} was flash frozen in liquid nitrogen and stored at −70 °C.

Solubilization of $PSII_{CC}$. Thirty milliliters of the frozen BBY sample was slowly thawed on ice. Melted sample was homogenized in a glass homogenizer, resuspended with 120 mL of buffer A (0.5 M sacharose, 40 mM MES NaOH, pH 6.0), and centrifuged for 30 min at 40000*g*. The pellet was resuspended in 18 mL of buffer B (1.8 M sacharose, 20 mM NaCl, 70 mM $MgCl_2$, 70 mM MES NaOH, pH 6.0), and centrifugation tubes were quickly rinsed with 12 mL of 10% *n*-octyl-β-D-glucopyranoside (w:w) into a glass homogenizer. The suspension was homogenized 15 times and left stirred on ice for 75 min. Then, 45 mL of buffer A was added and the suspension was centrifuged for 10 min at 48000*g*. The collected supernatant was combined with 93 mL of buffer C (40 mM MES NaOH, pH 6.0) and centrifuged for 1 h at 150000*g*. The volume of the collected supernatant was doubled by addition of buffer C, and the suspension was centrifuged for 30 min at 150000*g*. The pellet was resuspended in a buffer containing 0.02% β-dodecyl maltoside (β-DM) (w:w) and 50 mM MES NaOH, pH 6.5, flash frozen in liquid nitrogen and stored at −70 °C. The final concentration of the protein sample was 10−15 mg mL^{-1} equivalent to 2−4 mg (Chl *a*) mL^{-1}.

Purification of $PSII_{CC}$. The thawed $PSII_{CC}$ were purified first by continuous sucrose density gradient centrifugation (0−1 M sucrose, 1% β-DM, 50 mM MES NaOH, pH 6.5) at 90000*g* for 16 h. The second green zone from the top was collected and loaded onto an ion exchange column containing Q-Sepharose (Amersham Biosciences, Sweden). The column was washed by 50 mL of elution buffer (0.02% β-DM, 50 mM MES NaOH, pH 6.5, flow rate 2 mL min^{-1}). Extensive washing of the impurities was achieved by 200 mL of linear gradient of NaCl up to 400 mM (2 mL min^{-1}) in the elution buffer. The purified $PSII_{CC}$ was eluted following the 100−150 mL of elution buffer containing 400 mM NaCl (2 mL min^{-1}). This purified fraction was dialyzed against 0.02% β-DM, 10 mM $CaCl_2$, 50 mM MES NaOH, pH 6.5 overnight and spin concentrated at 2000*g* with a Centricons membrane filter with a 30 kDa cut off (Millipore, USA).

SDS−Polyacrylamide Gel Electrophoresis (SDS−PAGE). Purified $PSII_{CC}$ was solubilized in a loading buffer containing 3% SDS and 5% β-mercaptoethanol. Five microliters of the sample equivalent to 0.8−1.2 mg (Chl *a*) mL^{-1} was incubated for 5 min at 60 °C (optimized by screening of a temperature (30−100 °C) and time (1−60 min) of incubation). Four to six freshly grown crystals with dimensions of 200 × 200 × 50 μm were removed directly from the crystallization drop by nylon loops (Hampton Research (HR), Aliso Viejo, USA), washed in the corresponding precipitant, and solubilized in the loading buffer as the $PSII_{CC}$. Protein samples were loaded onto the denaturing SDS−PAGE with a 17.5% polyacrylamide gel.[23] The gels were stained using Coomassie Brilliant Blue R-250.

Crystallization. Crystallization experiments were setup using freshly purified protein at a concentration of 2−4 mg (Chl *a*) mL^{-1}. Protein was always manipulated in a room weakly illuminated with fluorescent light fitted with green filters (740 Aurora Borealis Green, Lee Filters, UK, $T_{MAX(525-575\ nm)} < 10\%$, $T_{MAX(700-750\ nm)} < 40\%$). Various precipitants with buffers ranging from pH 3 to 10 (citric acid, glycine, MES, imidazole, 4-(2-hydroxyethyl)-1-piperazine-ethanesulfonic acid (HEPES), PIPES, sodium acetate, sodium citrate, sodium HEPES, Tris hydrochloride, Tris, KH_2PO_4 and tricine), 1−350 mM divalent cations (Ba^{2+}, Mg^{2+}, Ca^{2+}, Mn^{2+}, Fe^{2+}, Cu^{2+}, Co^{2+}, Cd^{2+}, Be^{2+}, Zn^{2+}, Y^{2+}, Ni^{2+}, and Sr^{2+}), 5−60% (w:w) polyethylenglycols (PEGs) with various molecular weights (400, 3350, 4000, 6000, 8000, and 20000, and different combinations of them), 10−1000 mM inorganic salts (ammonium sulfate, ammonium acetate, sodium chloride, sodium citrate, sodium nitrate, sodium formate, and lithium acetate), 5−70% (w:w) organic agents (glycerol, 2-methyl-2,4-pentanediol (MPD), isopropanol, mannitol and ethylene glycol) as well as all 24 types of detergents with concentration 0.01−0.1% (w:w) from Detergent Screen 1 (Hampton Research (HR), USA) were screened for crystallization of $PSII_{CC}$. Also, conditions that have been successfully used for crystallization of thermophilic cyanobacterial PSII[5−13,24] were tested and modified (Table S1, Supporting Information).

Vapor-diffusion crystallization experiments were performed using the sitting and hanging drop techniques by mixing both protein and precipitant solutions.[25] Sitting drop crystallization was performed in 24 and 96 well plates (Figure 2c) (HR and Emerald BioSystems, USA). Hanging drop crystallization was carried out in 24 Linbro well plates (HR, USA) (Figure 2b). Reservoirs contained 200−1000 μL of crystallization reagents and droplets consisting of 4 μL of total volume with various precipitant−protein compositions (1:1, 1:2, 2:1, and 3:2).

Counter-diffusion crystallization experiments[26,27] were set up in glass capillaries (Figure 2e) of 75 mm length and inner diameters ranging from 0.1 to 0.5 mm (Hirschmann, Germany) using the three-layer configuration. Protein solution separated from the 30 μL of precipitant solutions by a 5 μL layer of 0.05−0.1% (w:w) low melting point agarose was placed in a sealed capillary and incubated in the Granada Crystallization Boxes (GCB, Triana Sci&Tech, Granada, Spain).

The Douglas Instruments, USA Vapor Batch 96 well plates (Figure 2a) were used to perform microbatch under oil method.[28] Various precipitants and protein solutions were mixed directly in the well to a final volume of 4 μL under a 2−3 mm oil layer. Paraffin and silicon oils (50:50 v:v) were used to seal the drops while allowing a slow evaporation rate.

Alternative crystallization procedures based on the use of divalent cation salts (Ba^{2+}, Mg^{2+}, Ca^{2+}, Mn^{2+}, Fe^{2+}, Cu^{2+}, Co^{2+}, Cd^{2+}, Be^{2+}, Zn^{2+}, Y^{2+}, Ni^{2+}, and Sr^{2+}) as additives were carried out on sitting and hanging drop methods. Single additive crystallization experiments were performed by mixing 0.1−1 μL of salt solution with 2 μL of protein−precipitant drop (1:1) using the hanging drop vapor-diffusion technique.

Cross-influenced procedure used a combination of different divalent cations at a final concentration of 2−5 mM in a multiple drop configuration as described.[29] In conventional hanging drop experiments additives were added directly to the protein−precipitant drop and to the reservoir, while in the cross-crystallization method additives were placed close to the protein−precipitant drop.

After loading the protein solutions into particular crystallization conditions, plates and/or boxes were covered by aluminum foil and stored at 4 and 19 °C. Later they were examined under the microscope (Olympus, SZ61 and SZX9, Japan) equipped with optical filters that block light in a range of 780−622 and 492−455 nm wavelengths (Olympus Optical CO Green Filter, HL3100-IF4, Germany).

Freshly grown crystals (1−3 days old) of $PSII_{CC}$ were mounted to the nylon loops (Hampton Research, Aliso Viejo, USA) and cryocooled in 100 K liquid nitrogen stream without additional cryoprotection. The crystals were tested for diffraction at the X13 beamline with a 0.801 Å monochromatic fixed wavelength in connection with the MARCCD 165 mm detector (DESY synchrotron in Hamburg, Germany), and at BM16 with the ADSC Q210r CCD detector (ESRF in Grenoble, France).

Results and Discussion

Initially, several *Pisum sativum* L. cultivars were tested to provide material for the optimal and reproducible crystallization procedure of the $PSII_{CC}$. Only the early spring varieties with broad dark green leaves suitable for biomass rather than seed production - 'Adept', 'Havel', 'Bohatyr', and 'Radovan' proved suitable for the PSII isolation. The cultivar 'Radovan' provided reproducibly the most stable PSII preparations and was therefore chosen for this study. The freshly isolated sample of $PSII_{CC}$ (in 40 mM MES-NaOH pH 6.5, 0.02% β-DM, and 1 mM $MnCl_2$) containing CP43, CP47, D1, D2, cytochrome b_{559}, all three subunits of OEC (PsbO, PsbP, PsbQ), and low molecular mass subunits (Figure 1) was used for our screening experiments with a wide range of crystallization techniques and conditions.

First, hanging and sitting drop vapor diffusion techniques and the published crystallization conditions (Table S1, Supporting Information) were used for the initial screening but did not facilitate any crystal growth. Very small green needle-shaped $PSII_{CC}$ crystals grew within 2−4 days at 23 °C using the hanging drop configuration with a modified precipitant solution containing 8% PEG 4000, 10 mM bis(2-hydroxyethyl)imonotris-(hydroxymethyl)-methane (Bis-Tris) pH 7.5, 10 mM ammonium sulfate, and 0.02% β-DM. Further optimization of the crystallization condition (see Experimental Section)

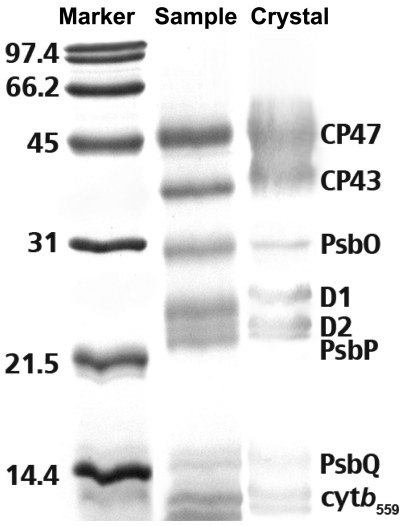

Figure 1. 17.5% SDS−polyacrylamide gel of $PSII_{CC}$. Both the freshly isolated sample and the dissolved crystals show an identical protein profile of intact PSII with all essential protein subunits present. The PSII protein subunits were identified according to their respective molecular masses. The low molecular weight proteins are not being resolved.

did not improve the crystal quality. In contrast, the addition of specific detergents (Deoxy-BigChap, LDAO, DDAO, HECAMEG, C-HEGA-10), buffers (citric acid, imidazole, sodium citrate, PIPES, glycine, sodium acetate), organic (MPD, isopropanol, ammonium acetate, sodium formate, lithium acetate) and inorganic agents (sodium nitrate), and the variation of the crystallization temperature (> 27 °C) prevented growth of any crystals.

Consequently, direct divalent cation crystallization experiments were performed. The divalent cations are involved in a number of oxidation−reduction processes including the electron-transfer in PSII. Here, the catalytic oxidation of water molecules by the OEC involves one calcium and four manganese ions. Ferrous ions are present in the iron−sulfur clusters of the cytochromes (ferric nonheme ion is indispensable for electron transfer between the quinons on the acceptor side of PSII), while magnesium is coordinated at the center of each chlorophyll ring.[30] Divalent cations also play an essential role in the stability of protein complexes through cation−anion interactions of amino acids residues. Specifically, manganese ions play an indispensable role for the stability of the OEC and hence the whole PSII. We have therefore conducted screening of a broad spectrum of divalent salts as additives to improve crystal quality and size. A combination of divalent cations in the cross-influenced experiments was tested as well. The results obtained from these experiments showed that the Fe^{2+}, Mn^{2+}, Mg^{2+}, and Ca^{2+} are the most effective divalent cations for crystal growth and have dramatically improved the crystal size (Figure 2). Among all of the ions that we have used, the presence of the Mn^{2+} cation (1−5 mM $MnCl_2$) in both the precipitant and the protein solution is absolutely necessary for the crystal formation process. Optimal concentration of the Mn^{2+} salt was determined after testing of several salt concentrations ranging from 1 to 10 mM in both protein and precipitant drops. Interestingly, the presence of the other above listed cations have a beneficial effect on crystals in cross-influence crystallization experiments but not when mixed directly with the protein solution in conventional hanging drop experiments.

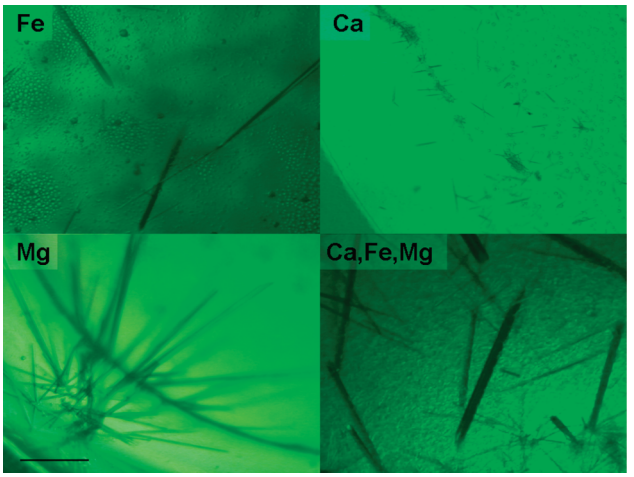

Figure 2. Crystallization of $PSII_{CC}$ with additive screening. Additive crystallization using a hanging drop vapor-diffusion technique with addition of 5 mM concentrations of Fe, Mg, and Ca ions added directly to protein−precipitant drop resulted in the precipitation with many small needles, precipitation with a needle cluster, and heavy amorphous precipitation with long single needles, respectively. The additive crystallization using a cross-influenced procedure (Mn as the main additive was added directly to the protein−precipitant drop well, while solutions of Ca, Fe, and Mg were separately placed in the other remaining wells of the sitting drop vapor-diffusion technique plate) promoted precipitation with long thicker needles. Scale bar represents 100 μm.

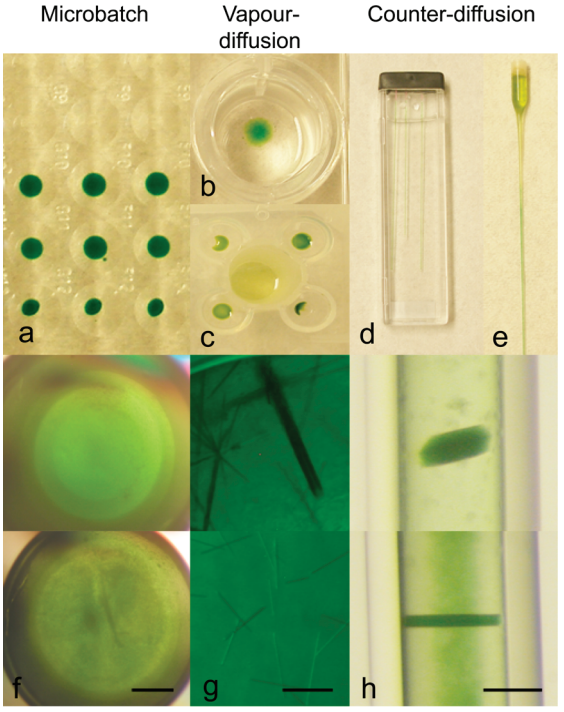

Figure 3. $PSII_{CC}$ crystallization. The microbatch crystallization (a) produced heavy amorphous precipitation (f), top - condition 1, bottom - condition 2. In the hanging (b) and sitting drop trials (c), crystals of $PSII_{CC}$ formed very flexible crystals with weak contacts in the aggregates (g - top) and many small aggregates (g - bottom), respectively. The crystals of $PSII_{CC}$ grown in the counter-diffusion experiment using the Granada crystallization box (d) and the single capillary (e) were well faceted with adequate shape. The crystals grown in the Granada crystallization box were of high quality (h - bottom) or even featuring 3D (h - top), diffracting to the resolution up to 1 nm. Scale bar represents 100 μm.

The second line of optimization was focused on improving crystal stability by reducing the $PSII_{CC}$ oxidation during the crystallization procedure. In vivo, the PSII suffers from oxidative stress by encountering free radicals such as singlet oxygen ($^1O_2$), superoxide anion ($O_2^{\bullet -}$), hydrogen peroxide (H_2O_2), and hydroxyl radical ($OH^{\bullet}$) that are scavenged by redox active enzymes (e.g., superoxide dismutase) but also by Chl *a*, carotenoids, quinones, and other antioxidant molecules.[31] The isolated $PSII_{CC}$ is not granted any such protection and hence is even more vulnerable to the oxidative stress. We have observed that the crystals grown by the vapor-diffusion were greatly unstable at room temperature with a degradation period of 2−5 days at 19 °C and one week when stored at 4 °C. A potent antioxidant, mannitol, was added to the precipitant solution in the vapor-diffusion experiments to prevent radical damage in combination with Ca^{2+}, Mn^{2+}, and Mg^{2+} salts. We observed that mannitol concentrations up to 0.5 M improved the crystal size. The largest crystals with dimensions of $70 \times 70 \times 800$ μm (Figure 3g) were obtained using a cocktail composed of 10% PEG 4000, 10 mM HEPES NaOH pH 7.5, 10 mM ammonium sulfate, 10 mM $CaCl_2$, 10 mM $MgCl_2$, 1 mM $MnCl_2$, 0.5 M mannitol, and 0.02% β-DM. Mounting of the needle-shaped crystals was complicated due their excessive flexibility and softness. Interestingly, the combination of PEG and high mannitol concentrations served as a cryoprotectant allowing for direct nitrogen stream cryocooling of crystals at 100 K without additional cryoprotection. The crystals were tested for diffractions at the X13 and the BM16 beamlines. Unfortunately, no X-ray diffraction was detected from any of these crystals indicating low order of the $PSII_{CC}$ in the crystal due to either the irregular packing or their inherent or degradation heterogeneity.

A possible explanation for the absence of diffraction is the $PSII_{CC}$ instability through the suspected oxidation of cofactors, proteins, and/or lipid molecules via ambient oxygen access to the protein−precipitant droplet in the vapor-diffusion crystallization technique. To overcome this problem and to crystallize $PSII_{CC}$, we moved into the counter-diffusion method as we have described previously.[32] Here, the precipitant and protein solutions are placed in a sealed capillary minimizing the oxidation damage of the photosynthetic sample. Yet the main advantage of the counter-diffusion method lies in the generation of a continuous supersaturation gradient without any vapor barrier within a single capillary. The capillary serves for simultaneous protein precipitation, nucleation, and crystal growth. In this way a wide range of precipitant conditions are screened at the same time in a single experiment.[26,27,33] This approach was applied for the $PSII_{CC}$ crystallization and produced stable well-shaped three-dimensional (3D) crystals with dimensions of about $180 \times 90 \times 50$ μm (Figure 3h). Different conditions were tested to find the optimal composition of precipitating solution. The best crystals were grown at 21 and 4 °C in 4−7 days under the following conditions: 15% PEG 4000, 50 mM Bis-Tris pH 7.0, 50 mM NaCl, 1 mM $MnCl_2$, and 0.02% β-DM. Interestingly, mannitol was not indispensable for the crystal growth under the set conditions. In addition, this cocktail was further used as a basic condition for testing the influence of divalent cations. 1−10 mM of each individual salt solution was directly mixed with the protein solution. However, we did not observe any beneficial effect on the crystal size and quality. The crystal composition was analyzed by SDS−PAGE of dissolved crystals versus the protein solution used for crystallization (Figure 1).

Crystals of the $PSII_{CC}$ grown in capillaries were tested for diffraction at the X13 and BM16 beamlines. The X-ray diffraction yielded isolated spots to a maximum resolution of 10.0 Å. The diffraction was strongly anisotropic with fiber-like diffraction at 90° of the observable highest resolution spots.

The microbatch procedure also commonly used for crystallization of oxygen-sensitive proteins was tested as a third crystallization method. The microbatch crystallization method prevents evaporation in small-volume experiments by the presence of oil and protects against "shock nucleation" caused during the mixture of high protein−precipitant concentrations.[28,34] Several crystallization conditions, which yielded crystals and improved crystal stability in previous experiments, were tested. Surprisingly, both condition 1 (10% PEG 4000, 10 mM HEPES-NaOH pH 7.5, 10 mM ammonium sulfate, 10 mM $CaCl_2$, 10 mM $MgCl_2$, 1 mM $MnCl_2$, 0.5 M mannitol, 0.02% β-DM) (Figure 2f top) and condition 2 (10% PEG 4000, 50 mM Bis-Tris pH 7.0, 50 mM NaCl, 1 mM $MnCl_2$, 0.02% β-DM) (Figure 2f bottom) yielded amorphous precipitation.

Finally, we reviewed additional factors that contribute to the improved crystal quality along with the previously screened physicochemical parameters. The sustainable functional and structural stability of the isolated $PSII_{CC}$ throughout the whole isolation, purification, and crystallization processes is imperative. The flawless life history of the plant, the finest health status at the time of biomass harvest and optimization of all the subsequent steps leading to the isolated $PSII_{CC}$ are of essential importance and dictate the complexes' homogeneity in all aspects. Instead of whole plant homogenization, selective harvest of single leaves with fully matured chloroplasts by hand picking from healthy plants will increase the reproducibility of $PSII_{CC}$ isolation and its homogeneity as in the successful crystallization of plant PSI.[35] From the crystallization screens, it also becomes clear that Mn^{2+} ions are vitally important for the $PSII_{CC}$ integrity, just as Ca^{2+} and Mg^{2+}. We therefore propose to include mM concentrations of the aforementioned divalent cations' chlorides in all buffers used during the isolation, purification, and crystallization procedures. The limited access of oxygen played also a significant role in granting prolonged stability of the isolated $PSII_{CC}$ in counter diffusion crystallization. Here, we were able to set the conditions for truly 3D crystals of plant $PSII_{CC}$ for the first time. Although the addition of reducing reagents (e.g., ferrocyanide, sodium dithionite, ascorbic acid) will not be desired in any of the buffers used, the use of an oxygen-free atmosphere and degassed buffers is advisable wherever possible. The use of filtered light preventing any excitation of PSII, low temperature at all times, and the presence of antioxidants and protease inhibitors in the early stages of the PSII isolation procedure are the well-known but often neglected conditions. The crystallization trial itself will have to be confined in a glovebox under an inert atmosphere. We are confident that the use of the identified physicochemical parameters and meeting the proposed conditions will significantly improve the crystallization conditions and will in time result in the growth of diffracting $PSII_{CC}$ crystals that will provide the first high resolution information about the plant PSII.

Conclusion

Screening of the conditions that have been successfully utilized for crystallization of the systems homologous to the $PSII_{CC}$ from *Pisum sativum* promoted no growth of crystals. The subsequent screening aiming to optimize a wide range of chemical additives revealed the presence of Mn^{2+} in both the precipitant and the protein solution is essential for crystal formation. The presence of other divalent cations (Ca^{2+}, Mg^{2+}, Fe^{2+}) has a beneficial effect on crystals in cross-crystallization experiments but has no or a limited effect in the direct mixtures with the protein solution in the conventional hanging drop experiments. The subsequent testing of the several crystallization techniques singled out the counter-diffusion method using the optimized content of divalent cations, namely, the Mn^{2+}, as the only conditions facilitating the growth of 3D crystals of $PSII_{CC}$ diffracting at 10.0 Å. We suggest this method as the best suited for the membrane protein crystallization trials, complementary to the standard vapor-diffusion techniques. We also concluded that the use of the alternative crystallization techniques renders better results compared to the sequential optimization experiments using a single method. In addition, we have also proposed new conditions for isolation and crystallization that will secure the stability of the $PSII_{CC}$ and will promote a growth of qualitatively distinct crystals. The new experimental design will take into account the $PSII_{CC}$ liability toward the oxidative stress, temperature, and light sensitivity and the presence of the indispensable divalent cations.

Acknowledgment. This work is supported by Grants NSM6007665808 and LC06010 of the Ministry of Education of Czech Republic, IAA608170901 of the Grant Agency of the Academy of Sciences of the Czech Republic, Institutional research concept AVOZ60870520, AV0Z50510513, AV0Z-50520514 and AV0Z40550506 of Academy of Science of Czech Republic, and the OptiCryst project of the Sixth Frame Work, UE. This is a product of the "Factoría Española de Cristalización", Consolider-Ingenio 2010 project (MEC). E.P.M. is supported by a "Ramón y Cajal" research contract (Spanish Ministry of Science and Technology). We are grateful to X13 (DESY synchrotron in Hamburg, Germany) and BM16 (the ESRF in Grenoble, France) staff for the support during crystals testing.

Supporting Information Available: Summary of crystallization conditions of membrane protein complexes from *Pisum sativum* L. and thermophilic cyanobacterium *Synechococcus elongatus* (Table S1). This material is available free of charge via the Internet at http://pubs.acs.org.

References

(1) Biesiadka, J.; Loll, B.; Kern, J.; Irrgang, K.-D.; Zouni, A. *Phys. Chem.* **2004**, *6*, 4733–4736.
(2) Anati, R.; Adir, N. *Photosynth. Res.* **2000**, *64*, 167–177.
(3) Kern, J.; Renger, G. *Photosynth. Res.* **2007**, *94*, 183–202.
(4) Zouni, A.; Kern, J.; Frank, J.; Hellweg, T.; Behlke, J.; Saenger, W.; Irrgang, K.-D. *Biochemistry* **2005**, *44*, 4572–4581.
(5) Kuhl, H.; Kruip, J.; Seidler, A.; Krieger-Liszkay, A.; Bünker, M.; Bald, D.; Scheidig, A., J.; Rögner, M. *J. Biol. Chem.* **2000**, *275*, 20652–20659.
(6) Zouni, A.; Witt, H.-T.; Kern, J.; Fromme, P.; Krauss, N.; Saenger, W.; Orth, P. *Nature* **2001**, *409*, 739–743.
(7) Kamiya, N.; Shen, J. R. *Proc. Natl. Acad. Sci. U.S.A.* **2003**, *100*, 98–103.
(8) Vasil'ev, S.; Brudvig, G. W.; Bruce, D. *FEBS Lett.* **2003**, *543*, 159–163.
(9) Ferreira, K., N.; Iverson, T., M.; Maghlaoui, K.; Barber, J.; Iwata, S. *Science* **2004**, *303*, 1831–1838.
(10) Suorsa, P.; Helle, H.; Koivunen, V.; Huhta, E.; Nikula, A.; Hakkarainen, H. *Eurasian Proc. R. Soc. Lond.* **2004**, *B 271*, 435–440.

(11) Kern, J.; Loll, B.; Lueneberg, C.; Difiore, D.; Biesiadka, J.; Irrgang, K.-D.; Zouni, A. *Biochim. Biophys. Acta* **2005**, *1706*, 147–157.
(12) Loll, B.; Kern, J.; Saenger, W.; Zouni, A.; Biesiadka, J. *Nature* **2005**, *438*, 1040–1044.
(13) Guskov, A.; Kern, J.; Gabdulkhakov, A.; Broser, M.; Zouni, A.; Saenger, W. *Nat. Struct. Mol. Biol.* **2009**, *16*, 334–342.
(14) Morris, E., P.; Hankamer, B.; Zheleva, D.; Friso, G; Barber, J. *Structure* **1997**, *5*, 837–849.
(15) Barber, J.; Nield, J.; Morris, E. P.; Zheleva, D.; Hankamer, B. *Physiol. Plant.* **1997**, *100*, 817–827.
(16) Boekema, E. J.; Roon, van, H.; Calkoen, F.; Bassi, R.; Dekker, J. P. *Biochemistry* **1999**, *38* (8), 2233–2239.
(17) Caffarri, S.; Kouřil, R.; Kereiche, S.; Boekema, E. J.; Croce, R. *EMBO J.* **2009**, *28*, 3052–3063.
(18) Suorsa, M.; Sirpio, S.; Allahverdiyeva, Y.; Paakkarinen, V.; Mamedov, F.; Styring, S.; Aro, E.-M. *J. Biol. Chem.* **2006**, *281*, 145–150.
(19) Rukhman, V.; Lerner, N.; Adir, N. *Photosynth. Res.* **2000**, *65*, 249–259.
(20) Nugent, C., I.; Hughes, T., R.; Lue, N., F.; Lundblad, V. *Science* **1996**, *274*, 249–252.
(21) Tsiotis, G.; Walz, T.; Spyridaki, A.; Lustig, A.; Engel, A.; Ghanotakis, D. *J. Mol. Biol.* **1996**, *259*, 241–248.
(22) Ghanotakis, D. F.; Demetriou, D. M.; Yocum, C. F. *Biochem. Biophys. Acta* **1987**, *891*, 15–21.
(23) Laemmli, U. K. *Nature* **1970**, *227*, 680–685.
(24) Adir, N. *Acta Crystallogr.* **1999**, *D55*, 891–894.
(25) Bergfors, T. M. International University Line: La Jolla, CA, 1999.
(26) Garcia-Ruiz, J. M. *Methods Enzymol.* **2003**, *368*, 130–154.
(27) Gavira, J. A.; Jesus, W.; Camara-Artigas, A.; Lopez-Garriga, J.; Garcia-Ruiz, J. M. *Acta Crystallogr.* **2006**, *F62*, 196–199.
(28) Chayen, N. E. *J. Cryst. Growth* **1999**, *196*, 434–441.
(29) Tomcova, I.; Kuta-Smatanova, I. *J. Cryst. Growth* **2007**, *306* (2), 383–389.
(30) Shcolnick, S.; Keren, N. *Plant Physiol.* **2006**, *141* (3), 805–810.
(31) Adir, N.; Zer, H.; Shochat, S.; Ohad, I. *Photosynth. Res.* **2003**, *76*, 343–370.
(32) Kutá-Smatanová, I.; Gavira, J. A.; Řezáčová, P.; Vácha, F.; García-Ruiz, J. M. *Photosynth. Res.* **2006**, *90*, 255–259.
(33) Lopez-Jaramillo, F. J.; Garcia-Ruiz, J. M.; Gavira, J. A.; Otalora, F. *J. Appl. Crystallogr.* **2001**, *34*, 365–370.
(34) D'Arcy, A.; Mac Sweeney, A.; Habera, A. *J. Synchrotron Radiat.* **2004**, *11*, 24–26.
(35) Ben-Shem, A.; Nelson, N.; Frolow, F. *Acta Crystallogr.* **2003**, *D 59*, 1824–1827.